Fermi National Accelerator Laboratory

FERMILAB-Conf-95/009-E

DØ

The DØ Detector at Fermilab: Recent Results and Future Plans

Jan S. Hoftun
For the DØ Collaboration

Brown University
Providence, Rhode Island 02912

Fermi National Accelerator Laboratory
P.O. Box 500, Batavia, Illinois 60510

January 1995

Presented at the *First Arctic Workshop on Future Physics and Accelerators*, Saariselka, Lapland, Finland, August 21-26, 1994

Operated by Universities Research Association Inc. under Contract No. DE-AC02-76CHO3000 with the United States Department of Energy

Disclaimer

THE DØ DETECTOR AT FERMILAB: RECENT RESULTS AND FUTURE PLANS

JAN S. HOFTUN
Brown University,
Providence, RI 02912
For the DØ Collaboration

ABSTRACT

The DØ Collaboration at Fermilab consists of about 400 physicists from institutions in 8 countries. The detector built by this collaboration has three main parts, a Central Detector, a liquid Argon - Uranium calorimeter and an outer muon detector. A very successful run was completed in May of 1993; analyses of this data are nearing completion and several physics results have already been presented. Another run started in January of 1994 and is still continuing. Some of the results from the first run, prospects for forthcoming physics results and plans for detector upgrades will be presented in this paper.

1. Detector

The DØ Detector at Fermilab is a large multipurpose detector used to study proton-antiproton (p-$\bar{p}$) collisions at the Tevatron Collider. The collider is the highest energy accelerator in the world, reaching a center-of-mass energy of 1.8 TeV. The detector is described in detail elsewhere[1]. A cutaway view of the detector can be seen in Fig. 1. It is separated into three subdetectors of different types and purposes. The emphasis in the design of the detector was on excellent electron and muon identification together with good solid-angle coverage, needed for a good measure of any missing energy in an event. There is no central magnetic field; this design choice permits the calorimeter and muon systems to be as compact as possible and avoids the extra amount of material in front of the calorimeter. The major features of each of the subdetectors, as well as of the trigger and data-acquisition system will be described briefly here. The coordinate system used to describe the detector and the interaction of particles inside it has the z-axis along the proton beam direction and its origin at the center of the detector (also as close to the center of the beam interaction region as possible). The other coordinates are x and y in the normal right-handed way (x outwards from the center of the accelerator and y vertical). Other coordinate variables used are the radius r which is the distance from the z-axis, azimuthal angle ϕ which is the angle with respect to the x-axis as defined above and the polar angle θ with respect to the z-axis. In many cases the pseudo-rapidity which is defined as $\eta = -ln[tan(\theta/2)]$, is used instead of the polar angle θ. This is a natural variable to use in describing the interactions since under a Lorenz boost, all particles are shifted by a constant $\Delta\eta$.

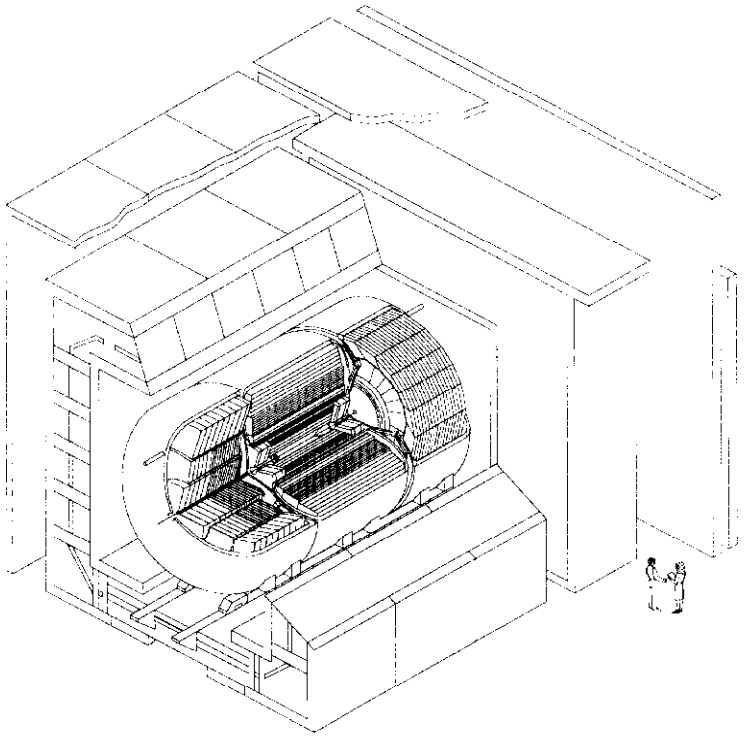

Fig. 1. DØ Detector.

1.1. Central Detector

The inner part of the detector is called the Central Detector and consists of four separate subsystems: the Vertex Drift Chamber (VTX), the Transition Radiation Detector (TRD), the Central Drift Chamber (CDC) and the Forward Drift Chamber (FDC). The VTX is a drift chamber with an inner radius of 2.7 cm and an outer radius of 16.2 cm. The resolution in $r\phi$ is 60 μm. The TRD is a stack of thin foils of polypropylene with a Proportional Wire Chamber to detect the X-rays emitted when high-energy electrons pass through the interface between polypropylene and the gas in the chamber. The TRD is used to improve the electron identification. The CDC is a drift chamber with inner radius 49.5 cm and outer radius 74.5 cm. The length is 184 cm. The resolution in $r\phi$ is 180 μm. The FDC is actually two chambers, one on each end of the detector. Each one is a sandwich of three drift chambers which measures θ and ϕ. The resolution is 200 μm.

1.2. Calorimeter

The calorimeter is separated into three different parts: a Central Calorimeter (CC) and two End-cap Calorimeters (EC). Each is housed in its own cryostat and for the most part consists of uranium plates and readout boards held apart with spacers. The volume between the plates is filled with liquid argon. In some parts of the calorimeter copper or iron is used as absorber instead of uranium. Each of the

three parts has an inner electromagnetic section, a fine hadronic section and an outer, coarse hadronic section. The calorimeter is as hermetic as possible, covering all solid angles out to $|\eta|$ of about 4. The readout is arranged in a tower-geometry pointing back to the interaction region, and in most cases the size of a readout tower covers a region in $\Delta\eta \times \Delta\phi$ of 0.1×0.1. The energy resolution of the calorimeter was measured in extensive test-beam runs and was found to be $15\%/\sqrt{E}$ for the electromagnetic section and $50\%/\sqrt{E}$ for the hadronic section.

1.3. Muon Detector

The muon detection system consists of five iron toroidal magnets and sets of Proportional Drift Tube chambers (PDT) for measuring positions on the muon tracks before and after the toroids. The magnetic field varies up to 2T in the magnetized iron. The coverage is out to $|\eta| < 3.3$ and the momentum resolution is $\delta p/p = \sqrt{0.2^2 + (0.01p)^2}$.

1.4. Triggers and Data Acquisition

The DØ trigger system is separated into three levels. The first (Level-0) is an interaction trigger using scintillator counters around the beam-pipe at each end of the detector. It senses inelastic collisions at a rate of about $2 * 10^5$ Hz. Next comes a dedicated hardware trigger (Level-1) which uses fast analog sums of energies, hits in muon chambers etc. to select interesting events. It has to make a decision in the 3.5 μsec separation between Tevatron bunches. The Level-1 trigger reduces the $2 * 10^5$ Hz input rate to around 150 Hz (some of these triggers require the confirmation by a slower hardware trigger (Level 1.5)). Following the hardware trigger the data from the entire detector is digitized. The final stage in the triggering system is a farm of processors (Level-2) where each computer receives a complete event over high speed data-cables from the front end digitizing electronics. The filtering in the Level-2 processors is done with computer programs written in high-level languages, and in many cases the algorithms used are subsets of the ones used for event reconstruction off-line. These filter algorithms run in a flexible "framework" which allows for easy changes of filter conditions (order of calls, cut parameters etc.) without remake of the filter program itself. The output rate from Level-2 to the host online cluster is about 4 Hz which is tuned to match the disk and tape recording capability of the host system.

2. Top Physics

The Standard Model (SM) of quarks and leptons describes the Weak, Electromagnetic and Strong interactions of these particles and the carriers of these interactions. Five quarks (q) have been verified experimentally so far; the up (u), down (d), strange (s) and bottom (b) quarks. This model requires the bottom quark to have an isospin partner which has been named the top (t) quark. There is some indirect evidence for such a quark from various measurements such as: the asymmetry of $e^+e^- \rightarrow b\bar{b}$, the

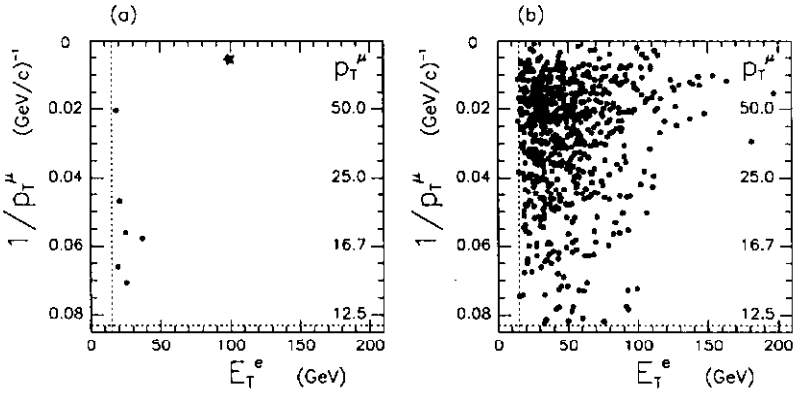

Fig. 2. Distribution of events in $1/p_T^\mu$ versus E_T^e for the data (before 2-jet requirement) (a) and for Monte Carlo generated $t\bar{t}$ events (b).

total and various partial widths of the Z^0 boson decay, the branching fraction for b to lepton pairs, the mass of the W boson and others. There is also reason to believe that the t-quark is very heavy. The currently published limit is 131 GeV/c^2 from the DØ collaboration[2].

The t-quark search is based on the fact that at the high energy of the Tevatron Collider (E_{CM} = 1.8 TeV) most of the t-quarks will be produced directly in the annihilation of $q\bar{q}$ (a few will also be produced by gluon-gluon fusion processes). In the CKM mixing matrix, the matrix element for t to b is essentially identical to one; thus the $(\bar{t})t$-quark decays to $(W^- + \bar{b})\ W^+ + b$ with a branching fraction of 100%. The search for the t-quark then may be done in several channels, depending on the decay of the W. The cleanest channels are the various dilepton ones, where both of the W's decay to leptons (e and/or μ) plus the associated neutrinos. The signature of these events is then the two leptons, missing transverse energy ($\not\!\!E_T$) from the neutrinos and the two b jets. The total branching fraction for all the combinations is about 5%. Another possible search channel has only one of the W's decaying leptonically whith the other W decaying into quarks. This would give a lepton, $\not\!\!E_T$ and 4 jets (2 from W decay + 2 b jets). The search in this decay channel may be further enhanced by looking for a soft lepton from the decay of one of the b or $\bar{b}$-quarks. The results reported on here come from the data taken during the 1992-1993 running period which had a total integrated luminosity of 13.5 pb^{-1}.

2.1. Dilepton channels

In the dilepton channel the three possibilities are $e\mu$, ee and $\mu\mu$. Many studies were performed to find the best variables to look at to try to separate background processes from the possible t-quark decay signal. In the $e\mu$ case, a plot of $1/p_T^\mu$ versus E_T^e from Monte Carlo generated data shows that the t-quark decay events populate the corner of small values of $1/p_T^\mu$ (high momentum) and large values of E_T^e while background processes generally have lower momentum for both the e and the μ. One

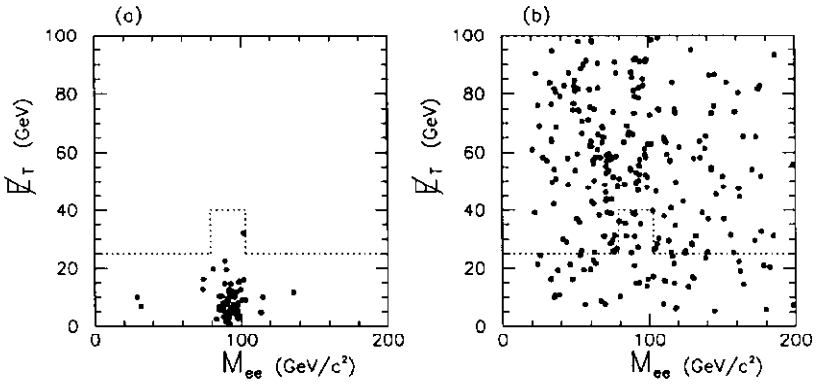

Fig. 3. Distribution of events in $\not\!\!E_T$ versus M_{ee} for the data (a) and for Monte Carlo generated $t\bar{t}$ events (b).

event survives the appropriate cuts in these variables (Fig. 2) as well as a cut requiring two jets in the event. In the ee channel a plot of $\not\!\!E_T$ versus the invariant mass of the two electrons is used (Fig. 3), and no events are found after the appropriate cuts are applied. In the $\mu\mu$ channel a plot of the azimuthal opening angle between the two muons versus $\not\!\!E_T$ is used together with the two jet requirement (Fig. 4), and again no events survive these cuts.

2.2. Semileptonic channels

For the semileptonic channels where the background is larger, several techniques have been used to extract the possible t-quark events. One method involves looking at the jet multiplicity. Jet multiplicity from background W+jet production follows a logarithmic scaling, when the number of events as a function of the number of jets in the event is plotted. This is shown in Fig. 5 which shows both W+jets and QCD multijet data and Monte Carlo generated events. The t-quark events in the leptons plus jets channel should have at least 4 jets as stated above and would show up as a deviation from this scaling in such a plot. Since the number of t-quark events is very small compared to the background jet production, this deviation is hard to see unless the selection is combined with the requirement of a b-quark tag of one of the jets, as described below. For the untagged data various event-shape studies have been performed. The first variable used to make shape cuts is aplanarity ($\mathcal{A}$) which is defined as 1.5 times the smallest normalized eigenvalue of the momentum tensor, which is constructed in the overall $\bar{p}p$ frame from the observed jets with $|\eta_{jet}| < 2$ in the event. The second shape cut variable is H_T, which is defined as the sum of the scalar transverse momenta of all final state jets observed in the event. The events with t-quarks will tend to be more spherical than the background QCD events and therefore have higher aplanarity. Since the jets in the t-quark events come from the decay of a heavy object, they will tend to have higher transverse momenta and therefore higher H_T. The cuts are set at $\mathcal{A} > 0.05$ and $H_T > 140$ GeV. The plots

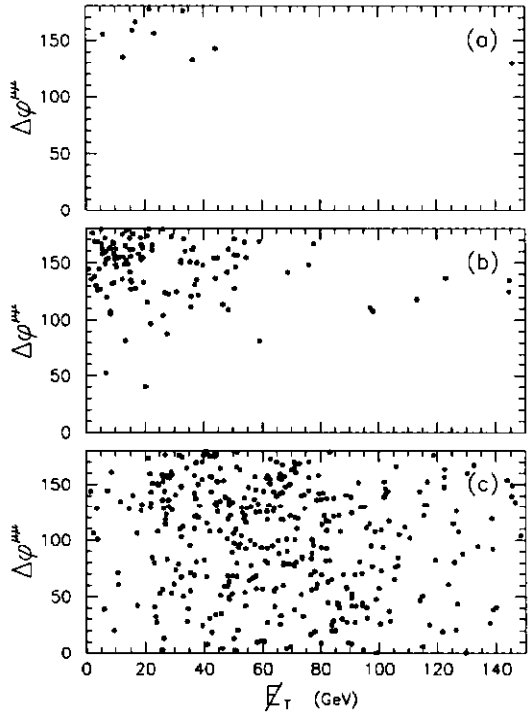

Fig. 4. Distribution of events in $\Delta\phi_{\mu\mu}$ versus $\not\!\!E_T$ for the data (a), for background $Z^0 \rightarrow \mu\mu$ from Monte Carlo generated events (b) and from Monte Carlo generated $t\bar{t}$ events (c).

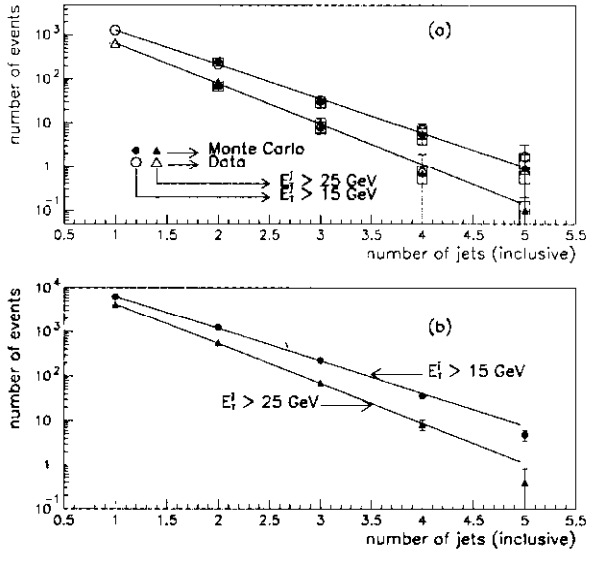

Fig. 5. Jet-multiplicity distributions of events from W + jets events (a) where the lines are fits to the data in the interval $1 < N_{jet} < 3$ and QCD multijet events from data and Monte Carlo generations (b) where the lines are fits to the data in the interval $1 < N_{jet} < 4$.

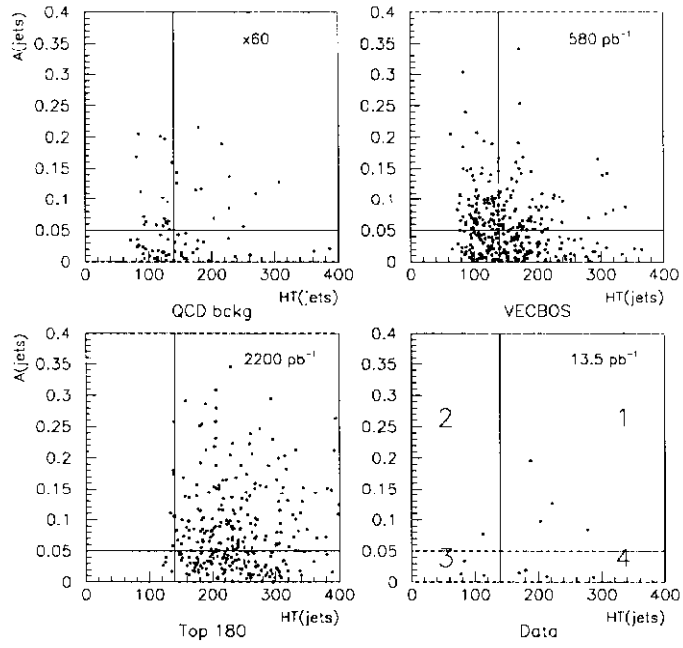

Fig. 6. Distribution of events in $\mathcal{A}$ versus H_T for Monte Carlo generated events and data as described in the text.

in Fig. 6 show the distributions in $\mathcal{A}$ versus H_T for scaled QCD background, W+jets Monte Carlo data, t-quark Monte Carlo data and finally the actually selected sample used to look for t-quark events. As can be seen from the figure, four events survive these two cuts, two each in the e+jets and in the μ+jets channels. As can also be seen from Fig. 6, there is a finite probability that these events come from the background channels. Two methods for estimating this probability have been used. The first uses the hypothesis of scaling behaviour of the W+jets (and QCD multijet) events. The number of background events with 4 or more jets can then be estimated from Monte Carlo calculations. This number is then corrected for the probability that the events will satisfy the $\mathcal{A}$ and H_T cuts. The resulting background estimate is 1.8 ± 0.9 events. The second method involves a fit to the fraction of the various processes which falls in each of the four quadrants on Fig. 6 with the number of signal events and of background events as free parameters. The result is a background estimate of 1.7 ± 0.9 events which agrees well with the first method above.

The final analysis focuses on the semileptonic channel where at least one of the b-quark jets is identified via a soft μ in the event. We report here only on the channel were the lepton in the W decay is an electron. In this case a simple background subtraction is performed. The background is assumed to follow the scaling in jet multiplicity mentioned above and the subtraction leaves two events above that background from the events with three or more jets. Other background left after the subtraction is estimated to be 0.6 ± 0.2 events.

m_t [GeV/c^2]		$e\mu$	ee	$\mu\mu$	e + jets	μ + jets	e + jets(μ)	ALL
140	$\epsilon \times B(\%)$	$.32 \pm .06$	$.18 \pm .02$	$.11 \pm .02$	1.2 ± 0.3	$.8 \pm 0.2$	0.6 ± 0.2	
	$\langle N \rangle$	$.72 \pm .16$	$.41 \pm .07$	$.24 \pm .05$	2.8 ± 0.7	1.3 ± 0.4	1.3 ± 0.4	6.7 ± 1.2
160	$\epsilon \times B(\%)$	$.36 \pm .07$	$.20 \pm .03$	$.11 \pm .01$	1.6 ± 0.4	1.1 ± 0.3	0.9 ± 0.2	
	$\langle N \rangle$	$.40 \pm .09$	$.22 \pm .04$	$.12 \pm .02$	1.8 ± 0.5	0.9 ± 0.3	1.0 ± 0.2	4.4 ± 0.7
180	$\epsilon \times B(\%)$	$.41 \pm .07$	$.21 \pm .03$	$.11 \pm .01$	1.7 ± 0.4	1.2 ± 0.3	1.1 ± 0.2	
	$\langle N \rangle$	$.23 \pm .05$	$.12 \pm .02$	$.06 \pm .01$	1.0 ± 0.2	0.5 ± 0.2	0.6 ± 0.2	2.5 ± 0.4
Background		$.27 \pm .09$	$.16 \pm .07$	$.33 \pm .06$	1.2 ± 0.7	0.6 ± 0.5	0.6 ± 0.2	3.2 ± 1.1
$\int \mathcal{L}dt$ [pb^{-1}]		13.5 ± 1.6	13.5 ± 1.6	9.8 ± 1.2	13.5 ± 1.6	9.8 ± 1.2	13.5 ± 1.6	
Data		1	0	0	2	2	2	7

Table 1. Efficiency $\times$ branching fraction ($\epsilon \times B$), expected number of events ($\langle N \rangle$) for signal and background sources for the observed integrated luminosity ($\int \mathcal{L}dt$), and number of events observed in the data.

2.3. Summary of Top Quark Search

All the results for the t-quark search are summarized in Table 1. Some of the channels are using less than the total available integrated luminosity due to changing trigger conditions during the run. The final result is seen to be 7 events with a background of 3.2 ± 1.1 events. Using this result for the various possible t-quark masses, the cross section for t-quark production is given in Fig. 7, which also has the value of cross section and mass from the published paper by the CDF collaboration[3]. The figure shows that even though the CDF cross section is higher than the one measured by DØ, they do agree within the error bars. As of this writing a final result from the data taken during the first run, including searches in other t-quark decay channels, has been submitted for publication[4]. Both DØ and CDF are currently collecting data, and further analysis of the previous data sample as well as the new will hopefully determine the mass and cross section for the t-quark.

3. New physics

Several searches for new particles and other phenomena which would point to physics beyond the standard model are being actively worked on by members of the DØ collaboration. Some of these analyses have already yielded results worth mentioning.

3.1. Leptoquarks

Leptoquarks are particles which appear in extended gauge theories as well as in some composite models. They connect the quark and the lepton sectors by carrying both baryon number and lepton number, and have fractional electrical charge and QCD color charge. Each leptoquark connects just one generation in the quark-lepton hierarchy, so there would be a total of three leptoquarks. At the Tevatron collider leptoquarks would be produced in pairs and then decay to a quark and a lepton of the appropriate generation. For the first generation the signature would then be two jets plus either two electrons, one electron plus $\not\!\!E_T$ from one neutrino or just $\not\!\!E_T$

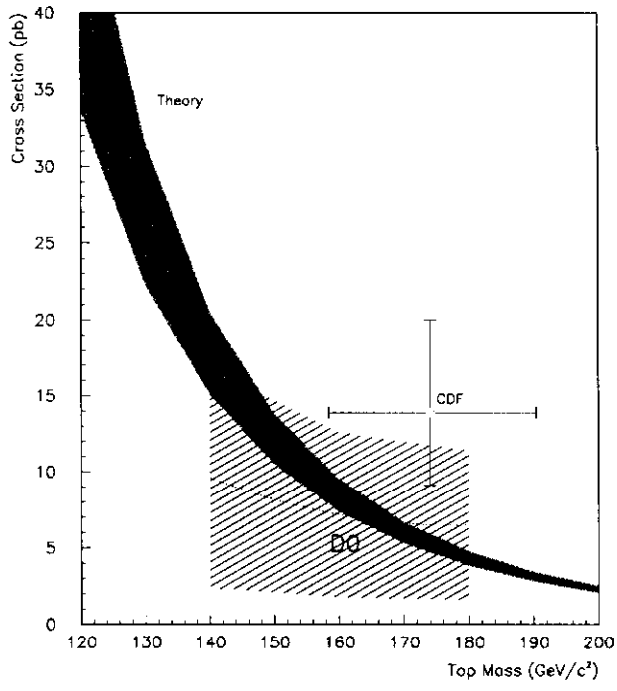

Fig. 7. Cross section for t-quark production from DØ with the CDF result added.

from two neutrinos. After all the appropriate cuts to remove background events, no events survive as leptoquark candidates. The limit on the mass of this particle is then dependent on its branching fraction to electron (β) where the branching fraction to neutrino is $1 - \beta$. The leptoquarks could be either scalar or vector particles. The results for the first generation as well as for the second generation (muon sector) are summarized in Table 2. The parameter κ describes a possible anomalous coupling of the leptoquarks to other particles. $\kappa = 1$ would mean a pure gauge coupling while $\kappa = 0$ would mean an anomalous coupling with composite leptoquarks. Part of this search has already been published[5].

Generation	Type	β	κ	Mass limit (95% CL)
First	Scalar	1.0		> 133 GeV/c^2
First	Scalar	0.5		> 120 GeV/c^2
First	Vector	1.0	1	> 244 GeV/c^2
First	Vector	0.5	1	> 234 GeV/c^2
First	Vector	1.0	0	> 193 GeV/c^2
First	Vector	0.5	0	> 189 GeV/c^2
Second	Scalar	1.0		> 95 GeV/c^2
Second	Scalar	0.5		> 80 GeV/c^2

Table 2. Leptoquark Mass Limits

3.2. Supersymmetry mass limits

Several searches for the Supersymmetric partners to the quarks and leptons are also underway. Some preliminary results from these searches has yielded the result of $m_{gluino} > 157$ GeV/c^2 at 95% CL if the lightest squark is assumed to be very heavy and $m > 218$ GeV/c^2 at 95% CL if the squark and gluino masses are assumed to be the same. Searches are also being performed for the SUSY partners of the gauge bosons. These results have been presented at several conferences[6].

4. Other physics topics

The DØ collaboration has also presented several other interesting physics results such as in electroweak physics, b-quark physics and Quantum Chromo-Dynamics (QCD) physics. The cross sections for W and Z boson production has also been measured, and the results agree very well with the published CDF results. A measurement of the W boson mass is also being performed.

The measured cross section for J/ψ production also agrees well with CDF and both experiments measure values which are higher than the values predicted by theory. The cross-section for inclusive production of b-quarks has also been shown. A preliminary result for the measurement of $B_0\bar{B}_0$ mixing shows good agreement with earlier experiments.

In QCD physics, some results have already been published, such as a measurement of the so-called Rapidity Gap[7].

5. Future Upgrade

The Fermilab accelerator complex is currently being upgraded to be able to deliver much higher luminosities to the experiments. This is partially achieved by building a new pre-accelerator, the Main Injector, to replace the use of the old Main Ring and thereby increase the intensity of the accelerated beams, and partially by increasing the number of concurrent bunches of particles in the accelerator. To cope with this increased luminosity an ambitious program for upgrading the DØ detector has been underway for some time. The whole inner part of the detector (Central Detector) will be replaced. The new layout is shown schematically in Fig. 8. The major change is that DØ will have a central magnetic field for measuring the charge of particles. It is now possible to make the magnet small enough to fit inside the existing calorimeter. The detection elements consist of a Silicon Tracker, Scintillating Fiber Tracker and Preshower Detectors.

The electronics and trigger system also will have to be upgraded to handle the increased rate and the closer bunch spacing. The major part of the trigger upgrade will take part at the lower levels, Level-0 and Level-1.

Overall the detector as upgraded will be even better suited to do physics at the highest available center-of-mass energy. It will be able to do b-quark tagging by looking for the decay-vertex of the b-quark which will improve the search/measurements

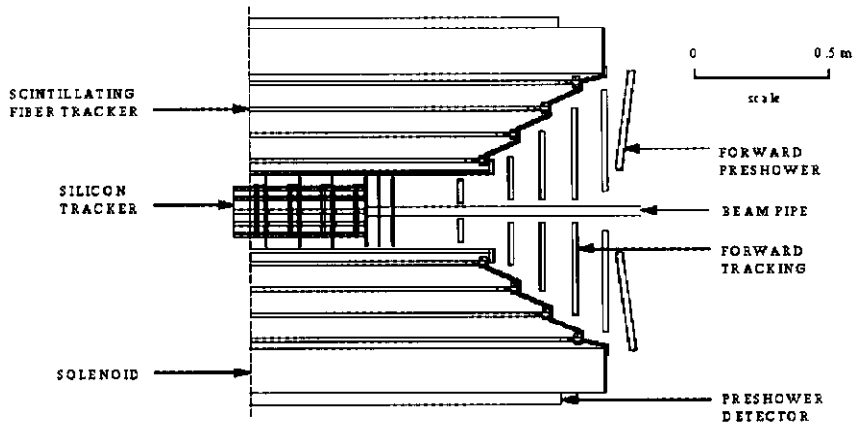

Fig. 8. Central Detector after upgrade.

for/of the t-quark.

6. Conclusions

The DØ detector is up and running very well. It has produced several results already in published form as well as many others either presented or very soon to come out. Much more data is available and more is being taken at a very good rate. The detector will be producing interesting physics results for many years to come, both in its current configuration and in its upgraded form later in this decade.

7. References

1. S. Abachi et al. (DØ collaboration), *Nucl. Instr. and Meth.* **A 338** (1994) 185.
2. S. Abachi et al. (DØ collaboration), *Phys. Rev. Lett.* **72** (1994) 2138.
3. F. Abe et al. (CDF Collaboration), *Phys. Rev. Lett.* **73** (1994) 225.
4. S. Abachi et al. (DØ Collaboration), *FERMILAB-Pub-94/354-E*, submitted to Phys. Rev. Lett.
5. S. Abachi et al. (DØ collaboration), *Phys. Rev. Lett.* **72** (1994) 965.
6. S. Hagopian. (DØ collaboration), to appear in the proceedings of the 27^{th} International Conference on High Energy Physics, Glasgow, Scotland (1994).
7. S. Abachi et al. (DØ collaboration), *Phys. Rev. Lett.* **72** (1994) 2332.